NMR SURFACE RELAXIVITY AND DIFFUSION EFFECTS IN GRAIN PACKS

S. Godefroy[1,2], J.-P. Korb[1], D. Petit[1], M. Fleury[2]

[1]Laboratoire de Physique de la Matière Condensée, UMR 7643 du CNRS,
Ecole Polytechnique, 91128 Palaiseau, France
[2]Institut Français du Pétrole, 92852 Rueil-Malmaison, France

Abstract

The surface relaxivity ρ is an important and fundamental parameter for the interpretation of T_2 distributions. To use laboratory data in the field, one must know the various effects that will influence ρ, such as temperature and mineralogy. Recent works suggest that ρ value is fluctuating more than expected and yields errors in water saturation estimation.

We studied low field (2.2 MHz proton) nuclear relaxation in calibrated silicon carbide (SiC) grain packs in a large range of grain size (8-150 µm) to avoid ambiguity due to pore size distribution of most consolidated reservoir rocks. To isolate the origins of surface relaxation, we varied the temperature from 85°C to 34°C. Measurements were performed with both high and low amount of paramagnetic impurities at the surface of the grains

When the amount of paramagnetic impurities is low, the surface relaxation is in the range of natural rocks and we found a linear relationship between T_1 and T_2 and pore size, indicating a relaxation process limited by the surface. When the temperature is increased, the linear relationship is still valid but there is a significant decrease of the relaxation times. Similar results obtained on porous silica glasses suggest that this unexpected phenomenon is due to a surface diffusion of proton species.

Introduction

Low field nuclear magnetic resonance is now routinely used to determine important reservoir properties such as porosity, water saturation and permeability. However, they are still important difficulties related to the determination of surface relaxivity. This fundamental parameter, linking the measured relaxation time T_2 to the surface-to-volume ratio (S/V) of the rock's porous space, can be determined by various methods and varies accordingly by several orders of magnitude. The most common method used is the comparison of T_2 distribution with mercury injection capillary pressure curves (MICP) because these measurements are simple and performed routinely for other purposes such as rock typing. However, the underlying strong assumption of a correlation between pore throats and pore bodies is only valid for 'simple' rocks for which conventional logging data may suffice. Therefore, such an approach cannot be generalized. Recent works confirm this expected weakness and indicate challenging questions about surface relaxivity; for sandstones, an extensive experimental study shows that the link between T2 and MICP is unpredictable (Lowden et al., 1998); for carbonates, Boyd and El Amam (1998) observed that the cut-off value used to calculate water saturation was not only higher than expected but varies by a factor of four for the samples studied. This implies that NMR logs can only be properly calibrated where cores have been taken for laboratory measurements and that the extrapolation of these calibrations to other intervals will be questionable, despite the various improvements of the logging tools.

Among possible techniques, pulsed field gradients NMR is a promising method to measure surface-to-volume ratio in rocks. However, the method is not straightforward and is limited to rocks with small internal gradients and a small amount of paramagnetic impurities. In a recent work, Hurlimann (1998) indicated that internal magnetic field gradients due to susceptibility contrast may be as large as 1000 Gauss/cm at 0.05 Tesla**.**

Nuclear magnetic relaxation methods are also very sensitive to paramagnetic impurities such as iron or manganese. Natural rocks contain variable amounts of impurities and this may lead to large differences between similar porous media and may explain partly the unpredictable results between T_2 and MICP, as reported by Lowden et al. (1998). Another important question is the temperature dependence of the surface relaxivity. This is of crucial importance because laboratory calibration experiments are usually not performed at reservoir conditions (for technical difficulties and cost). Contrary to bulk fluid, surface relaxation seems to depend weakly on temperature (Latour et al., 1992) in the practical range of hydrocarbon reservoir temperature (80-150 °C). However, further experimental evidence is required.

Our objective in this study is to identify the various mechanisms at the origin of the surface relaxivity in porous media where the pore sizes are known from the size of the grains used to build these media. Therefore, we avoid the difficulty of interpreting pore size distributions characterizing natural porous rocks which will be considered later. We studied proton nuclear relaxation on water saturated grain packs in various conditions of temperature and pore sizes in the range of interest for petroleum science. The grain packs were also prepared with both high and low amount of paramagnetic impurities at the surface of the grains.

Experiments

Materials

The different set of porous media were obtained by packing down silicon carbide (SiC) grains of same size. This material was found to be convenient to get model granular porous media, for many raisons. Firstly, packing yields reproducible porous media structure (Chauveteau et al. 1996), as described below. Secondly, the grain sizes, selected by sedimentation in air, are commercially available in a wide range. Thirdly, the surface properties are independent of the size. In addition, SiC grains have a sharp-edged shape, very similar to most sands (El Attar and Chauveteau, 1999).

Compared to other materials such as quartz, the surface characteristics of SiC are invariable with time. Hence, when flushing with acid, the surface is not modified and only paramagnetic impurities are removed. Though SiC is inert and chemically stable, about 25% of the surface of the grains (Medout et al.) is naturally covered by a silica coating (SiO_2), formed by passive oxidation with air oxygen. Therefore, the general behavior of SiC is close to that of silica (Coste, 1997). SiC density is 3.22 and its specific surface area determined by BET measurements ranges between 0.56 and 0.026 m^2/g (Table 1). BET values and scanning electronic microscopy observations indicate low roughness at small scale.

As a consequence of the geometrical properties of SiC, the grain packs only varying in pore size and permeability, not in porosity. The different porous media were packed in cells composed of a glass tube and two caps. The dimensions of the cells are 3 cm in diameter and 5 or 10 cm in length. The cells are connected to tubings for saturation and fluid injection. The saturation has been made under a vacuum of 5.10^{-4} bar with a water salinity of 5g/l (NaCl).

The porosity, measured by NMR (Table 1), is about 44% for all the samples except for the 8 µm grain pack sample (53%). For a given porosity, ϕ, the mean pore size, d_{pore} (Table 1), is deduced from the grain size, d_{grain}, according to :

$$d_{pore} \approx \left(\frac{\phi}{1-\phi} \right)^{1/3} d_{grain}. \qquad (1)$$

We show in Fig. 1 the grain size dependence of the permeability. The expected parabolic behavior is retrieved for such grain packs, as previously found (Table 1) (Nabzar et al 1997), indicating that the packing procedure is satisfactorily performed.

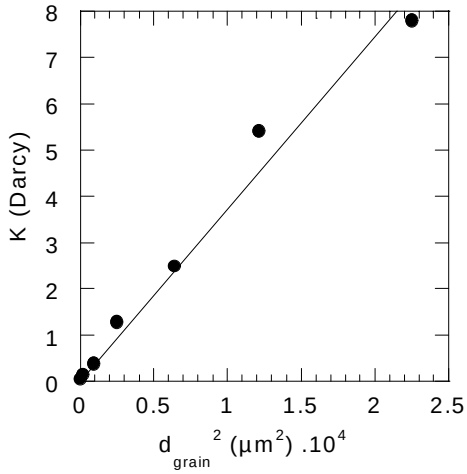

Fig. 1. Permeability of the various grain packs. The full line corresponds to the expected linear behavior.

Removing paramagnetic impurities

With the origin of ion impurities being uncertain, cleaning grain surfaces allows the performance of reliable surface relaxivity measurements. Preliminary results of electron spin resonance spectroscopy (ESR) on raw SiC grains exhibit a relatively high amount of paramagnetic impurities (Fe and Mn ions), probably at the surface of the grains. To remove these impurities, a cleaning has been performed by applying a continuous flux of HCl solution (1 mol/l) through the porous media. At the outlet of the cell, the acidic solutions were collected and analyzed by nuclear relaxation. The results are presented in Fig. 2 for the 50 µm grain pack. As the transverse relaxation rate $1/T_2$ is proportional to the paramagnetic ions concentration in solution (Bloembergen et al, 1948; Abragam, 1961), the sharp decrease of $1/T_2$, observed at short times, exhibits the removal of major impurities and iron fillings. The much slower decrease of $1/T_2$ observed at long times, shows the removal of the last impurities staying at the surface of the grains. After a few weeks, $1/T_2$ reaches asymptotically a plateau characteristic of the pure acid (about 0.5 s^{-1}), indicating the end of the cleaning procedure. However, this cleaning procedure does not remove impurities chemically bounded to silicon.

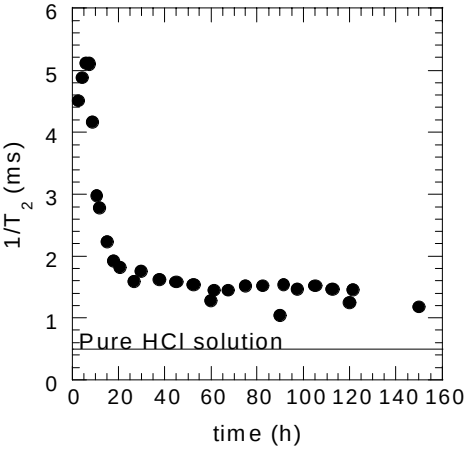

Fig. 2. Inverse of relation time of acidic solutions collected at the outlet of the 50 µm grain pack (34°C and 2.2 MHz). As $1/T_2$ is proportional to the paramagnetic ion concentration, the sharp decrease at short times shows the efficiency of the cleaning procedure.

NMR method

All proton NMR experiments were performed at 2.2 MHz on a Maran-2 spectrometer. This spectrometer allows the use of sample sizes up to 5 cm in diameter and 6 cm in length. The temperature of the probe is regulated at 34°C.

Longitudinal relaxation times, T_1, were measured by inversion-recovery sequence, using a signal-to-noise ratio of 50. Transverse relaxation times, T_2, were measured using the CPMG sequence. Due to electronic dead times, the minimum allowable half inter-echo spacing, τ, is 110 µs for the widest band pass of the filter, and 170 µs for the narrowest. The number of accumulations depends on the imposed signal-to-noise ratio (S/N ≈ 100 for measurement at 34°C and 50 for measurements with varying temperature).

The variations of T_2 with temperature were measured during a very slow decrease of the temperature of the thermally isolated cells from 85°C to 34°C. The duration of each scan is very fast compared to the time scale of temperature decrease. In the worst case, the variation of T_2 during the temperature decay is negligible. Moreover the weakness of the gradient fields rules out the effects of any possible induced temperature gradients, as discussed below.

For each sample, the narrow relaxation time distribution obtained by a multi-exponential fit (Fig. 3) is a clear signature of the narrow pore size distributions, for both uncleaned and cleaned samples. The presence of one or two very small peaks for all the samples studied, is still under investigation. However, these peaks represent less than 5% of the total volume and had no impact on our calculation. For all the data presented, we used a mono-exponential fit to determine the dominant relaxation time because such a calculation is more precise. We checked that T_2 obtained by a mono-exponential fit matches very well with the middle of the major peak of the distributions (Fig. 3), at any temperature.

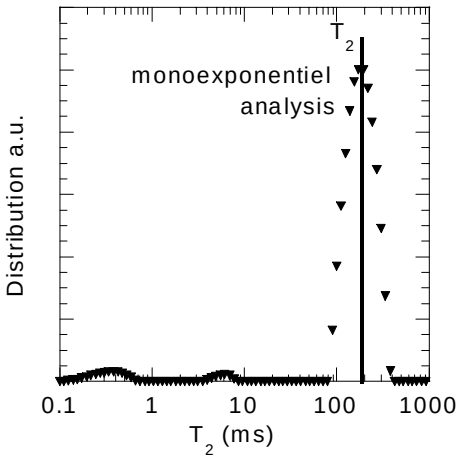

Fig. 3. Comparison between T_2 obtained by a mono-exponential fit and the T_2 distribution for the cleaned 8µm grain pack (2.2 MHz and 34°C).

Pore size dependence on nuclear relaxation

The linear pore size dependence of T_1 and T_2 is theoretically predicted and was shown experimentally for a range about two orders of magnitude smaller than those considered here (Korb et al. 1993). However, there is little experimental evidence in the size range of interest for petroleum sciences. A quadratic behavior might also be considered in certain conditions, as pointed out by Latour et al. (1992), and also discussed here.

Results

We investigated experimentally the relationship between pore size and relaxation time on both uncleaned (Fig. 4) and cleaned (Fig. 5) samples, to exhibit the effects of the paramagnetic species. The amount of paramagnetic species on the uncleaned surfaces is very high relatively to natural rocks, (as evidenced by the calculation of the surface relaxivity described later), and much lower on the cleaned ones, giving relaxation times an order of magnitude larger in cleaned packs. As a result, there is a net difference in the pore size dependence of the respective measured relaxation times T_1 and T_2 (Table 2). On the one hand, a quadratic behavior is observed for the uncleaned surfaces (Figs. 4). On the other hand for cleaned surfaces, the relaxation times tend towards the asymptotic value of the bulk $T_{1B}=T_{2B}$ (Fig. 5).

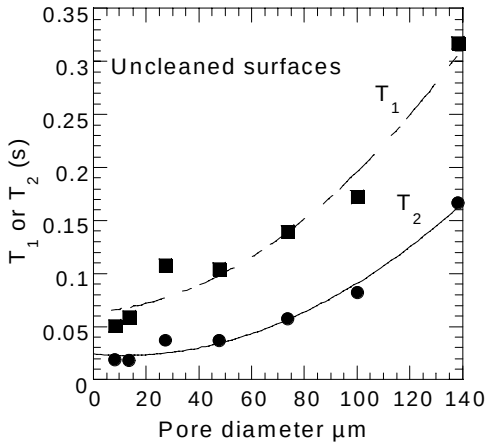

Fig. 4. Pore size dependence of the measured T_1 and T_2 (dots) for uncleaned surfaces (high amount of paramagnetic impurities), at 34°C and 2.2 MHz. The fits obtained with Eq. (5) show a quadratic behavior characteristic of the diffusion limited regime.

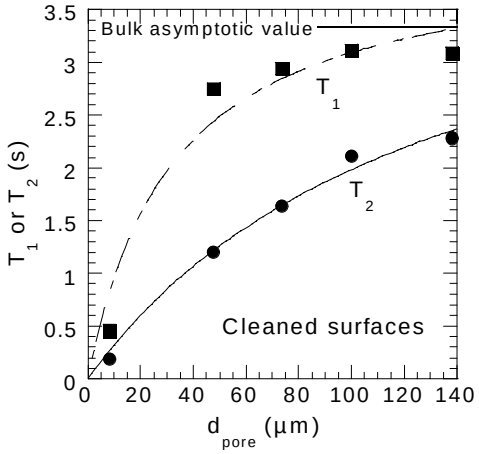

Fig. 5. Pore size dependence of the measured T_1 and T_2 (dots) for cleaned surfaces (low amount of paramagnetic impurities), at 34°C and 2.2 MHz. The fits obtained with Eq. (6) show the asymptotic value of the bulk.

Interpretation

From the first principles of nuclear relaxation of a liquid in a single pore, in the limit of the surface-volume fast exchange model, one can write after some calculations :

$$\frac{1}{T_{1,2}} = \frac{1}{T_{1,2B}} + \left[\frac{d_{pore}}{2\alpha} \frac{1}{\rho_{1,2}} + \frac{d_{pore}^2}{4\beta D} \right]^{-1} . \qquad (5)$$

In Eq. (5), ρ_1 and ρ_2 are the longitudinal and transverse surface relaxivities, respectively. D is the self-diffusion coefficient of the fluid. α is a shape factor (for our samples, a spherical shape can be taken, α=3). β includes the shape factor and other parameters (Brownstein and Tarr, 1979; Araujo et al., 1993). This equation does not account for the effect of field gradients on transverse relaxation time. Basically, there are two limiting regimes when comparing the surface relaxation time ($\propto d_{pore}/\rho_{1,2}$) to the time ($\propto d^2_{pore}/D$) needed to cross the pore by diffusion. When $\frac{\rho_{1,2} d_{pore}}{2D} << 1$ (Fast Diffusion Limit), one reaches the surface limited regime, where Eq. (5) becomes :

$$\frac{1}{T_{1,2}} = \frac{1}{T_{1,2B}} + \rho_{1,2} \frac{2\alpha}{d_{pore}}. \qquad (6)$$

In this regime the relaxation is limited by the rate at which the spins are relaxed at the pore surface. So $T_{1,2}$ vary linearly with the pore sizes. This approach is available for small pores, and/or low surface relaxivities. When $\frac{\rho_{1,2} d_{pore}}{2D} >> 1$ (Slow Diffusion Limit), one reaches the diffusion limited regime, where Eq. (5) becomes (Araujo et al., 1993) :

$$\frac{1}{T_{1,2}} = \frac{1}{T_{1,2B}} + \frac{4\beta D}{d^2_{pore}}. \qquad (7)$$

In this diffusion limited regime, the relaxation is limited by the surface access time. One notes that $T_{1,2}$ depend quadratically on the pore sizes. This is the case of large pores and/or high surface relaxivities. In the case of uncleaned samples, the bulk relaxation rate is negligible and the quadratic behavior seen on Fig. (4) is then characteristic of at least a contribution of the diffusion limited regime, depending on the pore sizes. When using the smallest pore, we estimate a value $\rho_2 \geq 37$ µm/s, confirming the diffusion limited regime for the large pores.

For the cleaned samples, the bulk relaxation rate (independent of the pore size) should be taken into account and we introduce the new variables T_{1corr} and T_{2corr} defined as :

$$\frac{1}{T_{1,2corr}} = \frac{1}{T_{1,2}} - \frac{1}{T_{1,2B}} = \rho_{1,2} \frac{2\alpha}{d_{pore}} \quad \text{(FDL)} \qquad (8)$$

When removing the bulk contribution $T_{1,2B}$ (eq. 8), the observed linear pore size dependence of $T_{1,2corr}$ shown in Fig. (6) confirms the FDL condition. When taking a spherical shape factor (α=3) in Eq. (8), we find ρ_2 = 3.4 µm/s. If one consider instead the specific surface (BET) measurements (table 1) to avoid considering a shape factor, we find ρ_2 = 1.7 µm/s. A calculation using mercury injection curves (not shown) yields ρ_2 = 0.7 µm/s (the pore throats are about 5 times smaller than the pore bodies). In any case, these surface relaxation values are in the range of those of natural rocks (Lowden et al. 1998), unlike the value obtained for uncleaned samples. The values of $\rho_2 d_{pore}/2D << 1$ presented in Table 2 were calculated using BET measurements and validate the surface limited regime for the set of cleaned samples. This clear verification of such a

model will strongly orientate our study on surface relaxation processes on cleaned samples. For most of the oil bearing rocks, Latour et al. (1992) suggested that the surface limited regime is applicable.

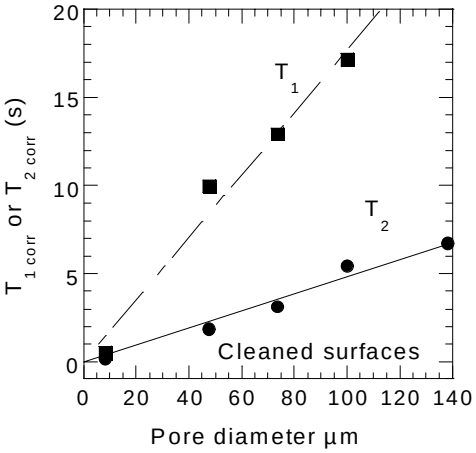

Fig. 6. Pore size dependence of T_{1corr} and T_{2corr} (dots) for cleaned surfaces, at 34°C and 2.2 MHz. The linear fits obtained validate Eq. (8) (FDL model). This allows a determination of the surface relaxivity ρ_2 = 1.7 µm/s .

Permeability

Due to the pore size dependence of the permeability (Fig. 1) and the corrected relaxation times T_{2corr} (Fig. 6), we retrieve the expected quadratic correlation between the permeability K and T_{2corr} (Fig. 7).

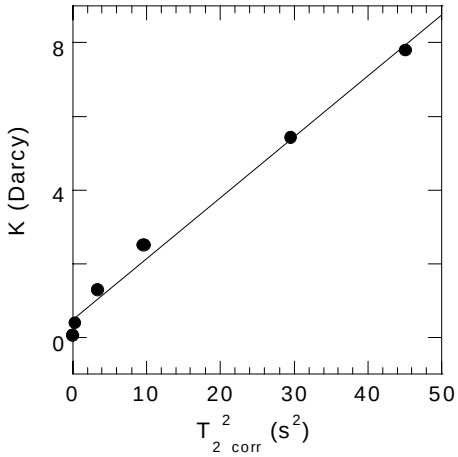

Fig 7. Quadratic correlation between the permeability and the corrected relaxation times for the cleaned samples.

Internal field gradient effects on nuclear relaxation

Up to now, we have neglected the field gradient contribution in the interpretation of our experiments due to a low inter-echo spacing. In this section we validate our assumption that the effects of internal gradients are negligible for our cleaned samples. It is known that the difference of susceptibilities between solid materials and fluids leads to microscopic internal gradients. Effect on T_2 will follow the relation :

$$\frac{1}{T_2} = \frac{1}{T_{2B}} + \rho_2 \frac{2\alpha}{d_{pore}} + \frac{D}{3}(\gamma \tau G)^2, \qquad (9)$$

γ being the gyromagnetic ratio of the proton, G the internal field gradient and τ the half inter-echo time spacing of the CPMG sequence. Fig. 8 shows the behavior of the observed relaxation rates $1/T_2$ *vs* τ^2, for different sizes of grain packs. The shape of the curves is almost similar for all the samples.

The non linearity observed is explained below with the consideration of restricted diffusion. It has been shown that the effective diffusion coefficient, D_{eff}, of fluid in pores depends on time through the inter-echo spacing, according to the relation (Latour et al., 1993) :

$$\frac{D_{eff}(\tau)}{D_0} = 1 - 0.22 \frac{2\alpha}{d_{pore}} \sqrt{2 D_0 \tau}\ , \qquad (10)$$

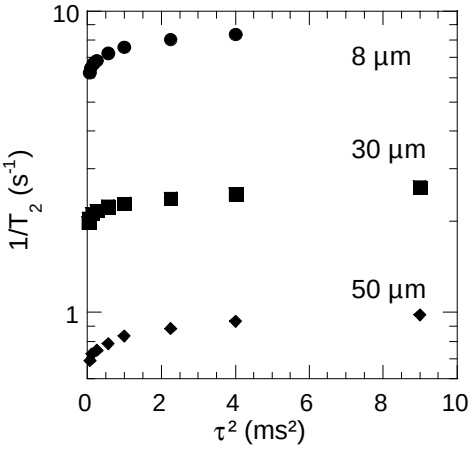

Fig. 8. Variation of the observed transverse relaxation rate with inter-echo spacing of the CPMG sequence for a 8, 30 and 50 µm grain packs at 34°C and 2.2 MHz.

where D_0 is the bulk diffusion coefficient. For large echo spacing, $D_{eff}(\tau)$ reaches an asymptotic value. Substitution of Eq. (10) into Eq. (9) gives thus at short τ :

$$\frac{1}{T_2} = \frac{1}{T_{2B}} + \rho_2 \frac{2\alpha}{d_{pore}} + \frac{D_0}{3}\left(1 - 0.44\alpha \frac{\sqrt{2 D_0 \tau}}{d_{pore}}\right).(\gamma G \tau)^2 . \qquad (11)$$

Eq. (11) explains the net deviation from linearity in Fig. 8. In the very short time range ($\tau \leq 500$ µs), the length of diffusion being much smaller than the pore size, Eq. (11) simplifies (the effective diffusion is the molecular diffusion) and we can estimate the gradients G, using different values of τ and eq. (9). Their values, presented in Table 3, range from 3.2 G/cm for the largest pores to 19.6 G/cm for the smallest ones. We show in Table 3 that the gradient contributions in Eq. (9) are negligible in the temperature range studied.

Temperature effects on nuclear relaxation

In order to isolate the origins of nuclear relaxation and to study the interaction of water with the surface, we have systematically explored the temperature dependence of $1/T_2$ in water saturated samples of different pore sizes (Fig. 9). We made a similar measurement on bulk water which gives an activation energy E_a = 4.5 kcal/mol which is very close to free water (Fig. 9). Measurements in calibrated porous media yield a temperature dependence reversing gradually from bulk water variation when the pore sizes decrease (Fig. 9). We check that the linearity between T_2 and d_{pore} is maintained in the whole temperature range. This is a strong argument in favor of conserving Eq.(8) (FDL) at any temperature :

$$\frac{1}{T_2(T)} = \frac{1}{T_{2B}(T)} + \rho_2(T)\frac{2\alpha}{d_{pore}} \quad \Rightarrow \quad \frac{1}{T_{2corr}(T)} = \rho_2(T)\frac{2\alpha}{d_{pore}} \qquad (12)$$

As a consequence the temperature dependence obtained for $1/T_{2corr}$, after subtracting the bulk contributions (Fig. 10), only comes from the surface effects ($\rho_2(T)$). One notes that temperature slopes of surface relaxivities are nearly parallel for all the pore sizes studied, but paradoxically inverse to bulk water (Fig. 10). This gives activation energies, E_s, ranging from –2 to –2.8 kcal/mol. A modification of the inter-echo spacing only induces a small shift of the temperature variations of T_{2corr}. This is an additionnal evidence that internal gradients are negligible.

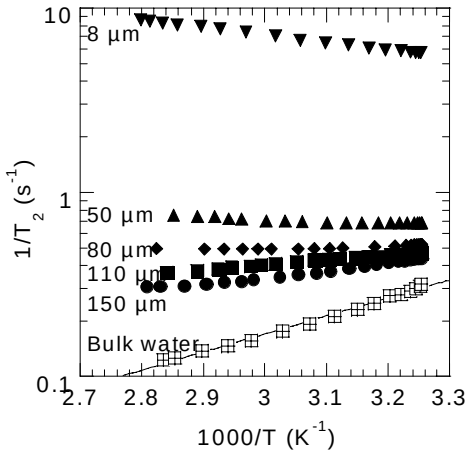

Fig. 9. Temperature dependence of the measured transverse relaxation times of water saturating the different samples and of bulk water (2.2 MHz). One notes that for bulk water, the exponential characterize activated process.

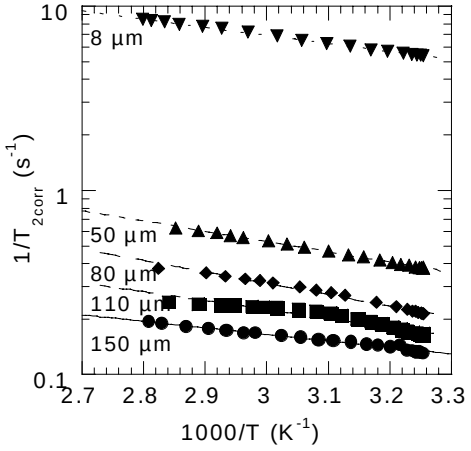

Fig. 10. Temperature dependence of the corrected transverse relaxation times of water saturating the different samples (2.2 MHz). The exponential fits of the curves points out activated processes.

A question now arises : what is the origin of the temperature dependence of $1/T_{2corr}$? The effects of weak gradient fields are ruled out because the activation energies deduced (Fig. 10) differ from that of diffusion ($-E_a$). The chemical exchange between bounded and bulk water near the pore surface might lead to similar temperature dependence but with a much larger activation energy. Moreover the verification of the condition of fast exchange allows us to exclude this process of relaxation. This behavior is paradoxical because it shows an increase of correlation time with increasing temperature. Recent proton NMR studies of water in calibrated nanoporous silica glasses have shown similar temperature results interpreted in terms of a particular proton species diffusion at the surface of the pore where paramagnetic species are present (Korb et al., 1997, 1999). In fact, at close proximity of paramagnetic impurity on the surface, the cluster of water in which the proton species diffuse, decreases in size when the temperature increases thus leading to a longer correlation time, leading to a shorter relaxation time (Korb et al., 1997, 1999). This process is of course limited by a chemical exchange with the bulk phase. Due to the similarity with the present experiments on calibrated porous media, we propose the same interpretation. The weak activation energy, E_s=-2.8 kcal/mol, is interpreted in fact as a difference between two activation energies : the one of free diffusion E_a, and the one, E_m, associated with the rate of

proton species chemical exchange in the surface layer.

Preliminary results on 100% oil (dodecane) saturated samples (50 µm) show that the temperature dependence of T_2 is nearly identical to bulk variation, with a positive activation energy. It suggests that the solid-liquid chemistry plays an important role in surface relaxation mechanisms.

Conclusion

We studied nuclear relaxation on water saturated calibrated SiC grain packs in various conditions of temperature (34-85°C) and pore sizes (8-150 µm) in the range of natural porous media. The limiting relaxation processes responsible for the observed data were evidenced, especially the surface relaxivity. The main results of this study are the following.

1. We found the expected linear relationship between T_1 and T_2 relaxation times and pore size when the amount of paramagnetic impurities is low. The calculated surface relaxivity is close to that of natural rocks. This validates the surface limited regime on such porous media and allowed the investigation of the surface relaxation mechanisms.
2. When the amount of paramagnetic impurities is low, the temperature dependence of the surface relaxation times T_2 was found to be inverse to that of bulk water. We have interpreted this paradoxical variation in term of a surface diffusion of proton species limited by the exchange with the bulk. If such a mechanism is confirmed on natural porous media, reservoir temperature should be taken into account when calibrating log data.

Further works are in progress to show that surface relaxation is very dependent on the surface chemistry.

Acknowledgments

We thank Dr. C. Chachaty (CEN Saclay) for the ESR measurements on our samples and Dr. G. Chauveteau (IFP) for helpful discussions on SiC material.

References

Abragam, A., 1961, The principles of nuclear magnetism: Oxford University Press, pp. 302-304

Araujo C. D., MacKay A. L., Whittall K. P. and Hailey J. R. T., ″A diffusion model for spin-spin relaxation of compartmentalized water in wood″, Journal of Magnetic Resonance, Series B 101, 248-261, 1993.

Bloembergen N., Purcell E.M. and Pound R.V., ″Relaxation effects in nuclear magnetic resonance absorption″, Phys. Rev., v.73, no.7, 1948.

Boyd D. and Medhat El Emam, ″Nuclear Magnetic Logging, does it meet expectations ?″, Proceeding of the 8th Abu Dhabi International Petroleum Exhibition and Conference, Abu Dhabi, UAE, 11-14 October 1998.

Brownstein, K.R., and Tarr, C.E., ″Importance of classical diffusion in NMR studies of water in biological cells″, Phys. Rev., Series A, v. 19, 1979.

Chauveteau G., Nabzar L., El Attar Y. and Jacquin C., ″Pore structure and hydrodynamics in sandstones″, SCA 9607, International Symposium of the society of Core Analyst, Montpellier, France, 8-10 Septembre 1996.

Coste J.-P., Ph. D. thesis, ″Dépôt de particules minérales de taille colloïdale en milieu poreux″, Université Paris VI, 1997.

El Attar Y. and Chauveteau G., ″Permeability control by colloid deposition″, in preparation.

Hurliman M. D., ″Effective gradients in porous media due to susceptibility differences″ Journal of Magnetic Resonance 131, 232-240, 1998.

Korb J.-P., Whaley-Hodges M. and Bryant R. G., ″Translational diffusion of liquids at surfaces of microporous materials : Theoretical analysis of field-cycling magnetic relaxation measurements″, Phys. Rev. E56, 1934, 1997.

Korb J.-P. and Bryant R. G., ″Anomalous surface diffusion of water in nanopores″, to be published in 1999 in Dynamics in small confining systems IV, Material research society.

Korb J.-P. and Bryant R. G., ″Anomalous surface diffusion of water compared to aprotic liquids in nanopores″ Accepted to Phys. Rev. E.

Korb J.P., Shu Xu and J. Jonas, "Confinement effect on dipolar relaxation by translationnal dynamic of liquids in porous silica glasses", J. Chem. Phys., 98, 2411,1993.

Latour L. L., Kleinberg R. L. and Sezginer A., ″Nuclear magnetic resonance properties of rocks at elevated temperatures″, Journal of Colloid and Interface Science, Vol. 150, No. 2, pp. 535-548, 1992.

Latour L. L., Mitra P. P., Kleinberg R. L. and Sotak C. H., ″Time-dependent diffusion coefficient of fluids in porous media as a probe of surface-to-volume ratio″, Journal of Magnetic Resonance, Series A 101, 342-346, 1993.

Lowden B.D. and M.J. Porter, "T2 relaxation time versus mercury injection capillary pressure: implications for NMR logging and reservoir characterization", Proceedings of the European Petroleum Conference, SPE 50607, The Hague, The Nederlands, 20-22 October 1998.

Medout-Marère V., A. ElGhzaoui, C. Charnay, J.M. Douillard, G. Chauveteau and S. Partika, "Surface heterogeneity of passive oxidized silicon carbide particles: hydrophobic-hydrophilic partition", submitted to J. Coll. Int. Sc., 1999.

Nabzar L, Coste J.-P. and Chauveteau G., ″Water quality and well injectivity″, 9th European Symposium on Improved Oil Recovery, The Hague, The Netherlands, 20-22 October, 1997.

Table 1. Samples characteristics				
Grain size (µm)	**Pore size (µm)**	**Specific surface (m^2/g)**	**Porosity (%)**	**Permeability (D)**
150	138.3		43.9	7.8
110	100		42.9	5.4
80	73.6		43.8	2.5
50	47.6		46.4	1.3
30	27.4	0.13	44.8	0.4
15	13.7	0.25	43.4	0.15
8	8.3		52.9	0.05

Table 2. NMR characteristics			
Pore size (µm)	**T_2 measured (ms) uncleaned surfaces**	**T_2 measured (s) cleaned surfaces**	**$\rho_2 d_{pore}/2D$ cleaned samples**
138.3	167	2.3	0.059
100	82	2.1	0.043
73.6	57	1.6	0.031
47.6	36	1.2	0.020
27.4	37		0.019
13.7	18		0.006
8.3	18	0.19	0.004

Table 3. Gradient and temperature effects on cleaned samples							
Pore size (µm)	**Gradient (G/cm)**	**τ (µs)**	**T_2 (s) measured (34°C)**	$\left[\frac{D}{3}(\gamma\tau G)^2\right]^{-1}$ **(s) (34°C)**	**T_2 (s) measured (79-83°C)**	$\left[\frac{D}{3}(\gamma\tau G)^2\right]^{-1}$ **(s) (85°C)**	$\left\|\frac{T_{2corr}(80°C)-T_{2corr}(34°C)}{T_{2corr}(80°C)}\right\|$ **%**
138.3	3.2	500	2.3	57	3.3	22	47.9
100	5.4	500	2.1	21	2.7	8	47.7
73.6	5.5	300	1.6	56	2.0	21	76.8
47.6	6.8	300	1.2	36	1.3	14	65.9
27.4	13.6	180		25		10	
8.3	19.6	220	0.19	8	0.12	3	56.9